GEOPHYSICAL RESEARCH LETTERS, VOL. 26, NO. 10, PAGES 1417-1420, MAY 15, 1999

A Validation Survey of the ECMWF Prognostic Cloud Scheme using LITE

S. D. Miller,[1] G. L. Stephens,[1] and A. C. M. Beljaars[2]

Abstract. Advancements in the parameterization of clouds in global circulation models (GCMs) are contingent upon our ability to validate them on the global scale. We examine the performance of the European Centre for Medium-range Weather Forecasting (ECMWF) prognostic cloud scheme using data from the Lidar In-space Technology Experiment (LITE). Qualitative comparisons and results from a statistical analysis are presented.

1. Introduction

Numerical weather prediction and climate modeling have represented historically two separate and distinct genres of discipline in the atmospheric sciences. The recognition of the latter as being a logical extension of the former has been stymied in practice by an inadequate representation of cloud, and hence cloud radiative feedbacks, in GCMs [see *Cess et al.,* 1990]. Clouds play an integral dual role in the dynamic climate system; acting not only in passive response (e.g., growth or decay) but also as physical drivers (in the context of diabatic heating). Proper representation of clouds in both capacities requires incorporating them into the model at the most fundamental level. This has stood as a formidable challenge to the improvement of forecasting skill, and by extension, climatology studies.

The intent of this study is to examine differences between cloud distributions as observed from an active remote sensor and those predicted in ECMWF forecasts matched to these observations. The choice to use ECMWF is based largely on the sophisticated nature of their cloud scheme and encouraging results of comparisons with surface radar observations [*Mace et al.,* 1997]. *Lau and Crane* [1995] use ISCCP cloud data and ECMWF analyses to examine the spatial and temporal variability of cloud, and *Klein and Jakob* [1998] extend this study to include a direct comparison between ECMWF composite simulations of frontal clouds with the ISCCP data. The current work differs significantly in the spatial scale at which high resolution cloud profile information are available to validate model forecasts.

2. The Data and Methodology

2.1. ECMWF cloud fields

ECMWF has taken an important step towards the realistic portrayal of cloudiness in GCMs in their employment of a prognostic cloud scheme. In contrast to diagnostic approaches, where clouds are considered essentially as byproducts of instantaneous environmental vectors of state, prognostic schemes represent clouds as evolving variables within the Earth-atmosphere feedback system. Described at length by *Tiedke* [1993] with revisions by *Jakob et al.* [1994], the scheme handles the full evolution of cloud with large-scale budget equations for cloud water/ice content. It considers their formation and dissipation in connection with turbulent forcing, entrainment of environmental air, diabatic and adiabatic heating/cooling, horizontal and vertical transport of cloud water and depletion by precipitation.

The ECMWF global spectral model uses triangular truncation at wavenumber 319, with 31 vertical model levels defined by hybrid coordinates (T319L31) and a reduced Gaussian grid of approximately 60×60 km. This grid is interpolated to 1-degree equal angle resolution for output purposes. Higher resolution is not necessary as the model fields are relatively smooth. Flux levels, which straddle the model levels, were used as the boundaries between adjacent profile bins. The focus of this study is the cloud fraction (CF) parameter, defined over the range of 0.0 (completely clear) to 1.0 (completely cloudy).

2.2. LITE cloud profiles

LITE [*McCormick et al.,* 1993; *Winker et al.,* 1996] flew aboard the Space Shuttle Discovery during September, 1994. Probing the atmosphere at near-nadir with a Nd-YAG lidar, LITE captured high resolution (15 m in the vertical and 0.74 km in the horizontal) details of the atmospheric profile heretofore unobtainable by passive satellite radiometers and with spatial coverage unavailable to terrestrial active sensors (Figure 1). For these intercomparisons the LITE cross sections, covering 7.4 km/s of ground track, are considered as “snapshots” of the global cloud field at a single ECMWF forecast step. Cloud boundaries were derived from these data using an signal-to-noise thresholding algorithm [*Winker and Vaughan,* 1994]. Night time orbits were selected, as their data are free of solar contamination in the 532 nm lidar detector channel [*Platt and Winker,* 1996].

2.3. Method outline

Short-range (24 to 30 hours) model forecasts were run to validate within 30 minutes of 15 different LITE orbit overpasses. ECMWF grid boxes along the flight tracks were identified and the model parameters and surface elevation were extracted. The resultant profiles to be compared with the LITE observations were comprised of adjacent grid boxes, with a variable amount of lidar information contained in each.

The LITE data were then binned to both the vertical (using the hypsometric equation and surface elevation to convert model hybrid flux levels to altitudes) and horizon-

[1]Department of Atmospheric Science, Colorado State University, Ft. Collins, Colorado
[2]European Centre for Medium-range Weather Forecasting (ECMWF), England

Paper number 1999GL900263.
0094-8276/99/1999GL900263$05.00

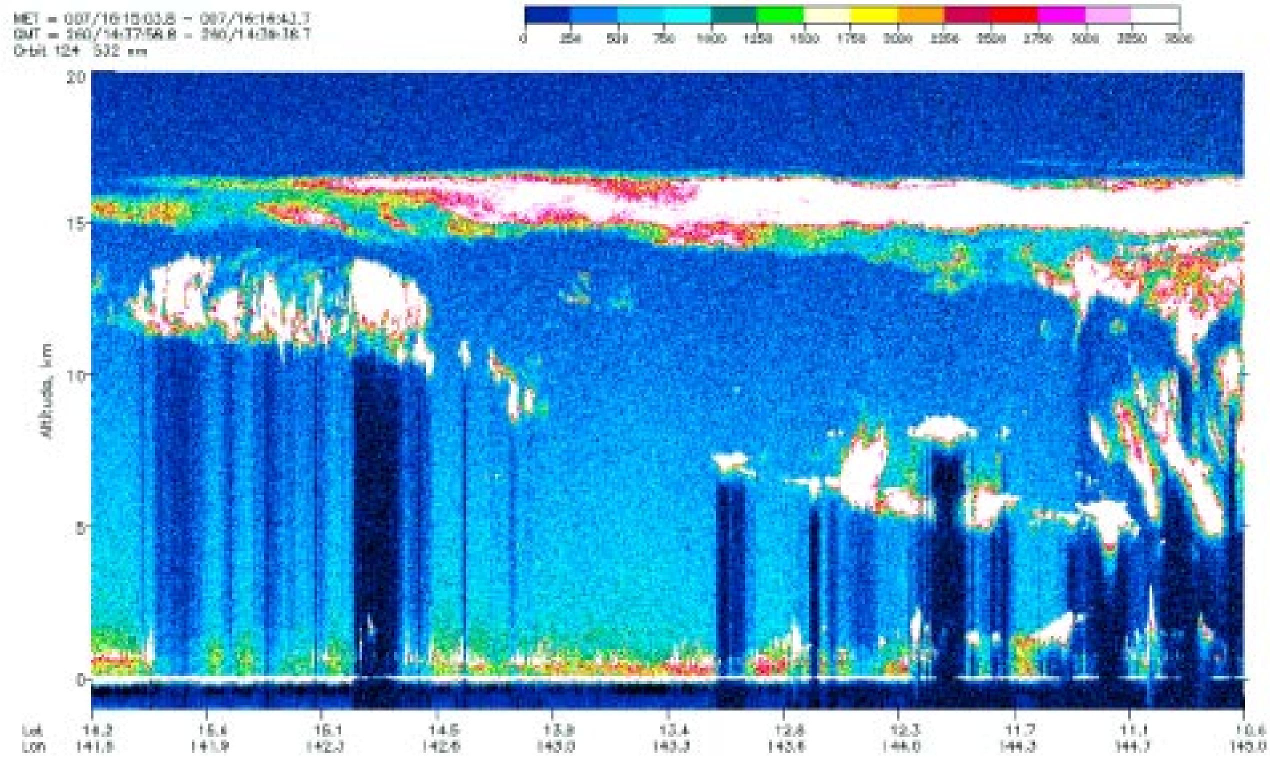

Figure 1. Example LITE cloud profile. (Image provided courtesy of NASA Langley Research Center)

tal (gathering all LITE profiles within a single grid box at each vertical bin) resolution of the model grid (Figure 2). A pseudo cloud fraction for the LITE data (CF_{LITE}) was computed for each level by normalizing the number of cloud profiles found by the total number of profiles in the grid box; done in an attempt to reconcile the differences between LITE's 2-dimensional slice and ECMWF's 3-dimensional "grid slice."

To assess model performance quantitatively, a statistical analysis analogous to *Mace* [1997] was performed. The following parameters characterize the analysis:

$$A = \text{cloud hit}, \qquad B = \text{false alarm},$$
$$C = \text{cloud miss}, \qquad D = \text{clearsky hit},$$

where (A, C, D) define agreements/disagreements between the model and observations and B classifies forecasts of cloud when the observations were clear. Because the amount of LITE cloud profile information in a model grid box varies according to the orbit path of intersection, the parameters are computed as

$$[A, B, C, D]^T = \sum_{i=0}^{N} P_i \cdot [A_i, B_i, C_i, D_i] \cdot [1., W_i, 1., 1.]^T,$$

where N is the number of ECMWF grid boxes spanned by the LITE orbit and P_i is the fraction of LITE profiles in the i^{th} grid box. To account in part for the sampling problem between LITE and ECMWF, false alarm contributions have been weighted (W_i) by cloud fraction in the following way. A model CF of unity is assessed a false alarm penalty having a magnitude of 1.0 - CF_{LITE}. Similarly, a non-zero model CF in clear sky observations is assigned a false alarm equivalent to the model CF (0$\rightarrow$1). As such, a small CF which may have existed within the grid box but outside the orbit cross section does not incur the full false alarm penalty.

The statistical definitions for hit rate (HR), threat score (TS), probability of detection (POD), and false alarm rate (FAR) [from *Wilks,* 1995] follow as

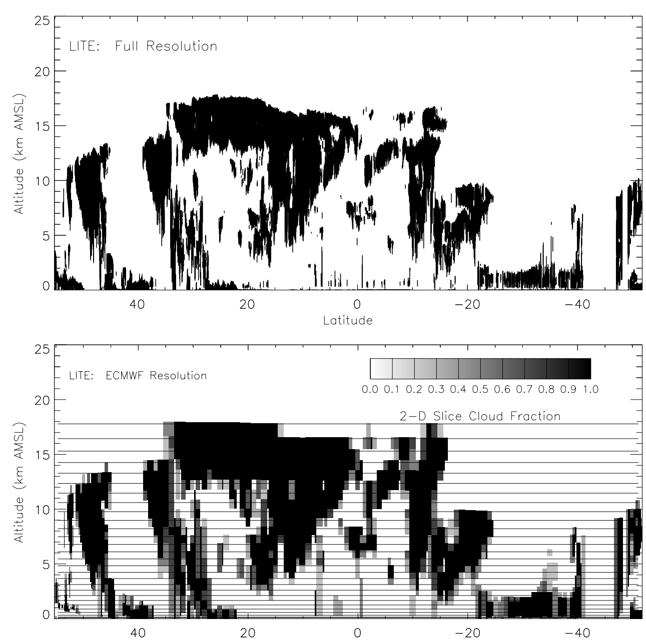

Figure 2. Recasting of high-resolution LITE (orbit 123) data to coarser ECMWF resolution. Averaged hybrid ECMWF vertical levels are indicated as horizontal lines in the lower panel.

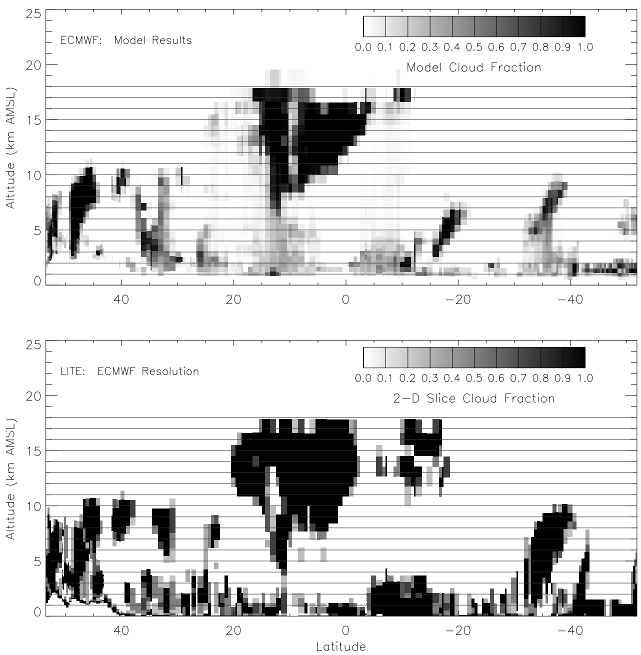

Figure 3. Cloud fraction comparison for LITE orbit 124 (September 16, 1994, 14:25-15:00 UTC, spanning the Western Pacific warm pool).

$$HR = \frac{A+D}{A+B+C+D}, \qquad TS = \frac{A}{A+B+C},$$

$$POD = \frac{A}{A+C}, \qquad FAR = \frac{B}{A+B} \quad .$$

HR is the fraction of correctly-forecasted (cloudy or clearsky) grid boxes, while TS excludes the clearsky component to focus only on the clouds. The ratio of cloud hits to the total number of *observed* clouds is given by POD, and FAR offers a metric for how often the model's cloud forecast was "crying wolf." A perfect forecast would thus entail HR = TS = POD = 1.0 and FAR = 0.0 (i.e., no misses or false alarms).

3. Preliminary Results and Discussion

An example of the ECMWF/LITE comparisons is shown for LITE Orbit 124 in Figure 3. Qualitatively, the vertical extent and placement of deep convection in the Inter-Tropical Convergence Zone (ITCZ), migratory mid-latitude disturbances, and large-scale subsidence zones appear to be in good agreement with the observations for this case. In light of the many discrepancies observed, this remains an encouraging commentary on our current abilities to represent the three-dimensional distribution of cloud in GCMs.

Table 1 presents the statistical results for all 15 model comparisons considered for this study. The "%" columns indicate the ensemble fraction of the data occupied by *any* amount of cloud, and the remaining columns contain the statistical figures outlined above. To address the possibility that a false alarm is in fact a "near-hit," a window of acceptance was applied to the intercomparisons and statistics re-computed. The results are included in Table 1 as parenthetical figures. The improvement in performance reflects the strong correlation observed by the naked eye in Figure 3 and indicates that, to within reasonable margins of error (e.g., ±1 model bins in the vertical as indicated in Figure 2), the model is forecasting the cloud distribution rather well.

Associated with the LITE data are caveats that warrant consideration. Some observations may possess an overestimate of the true cloud base altitude due to complete attenuation of the lidar pulse in the presence of optically-thick ($\tau > 10.0$) clouds. Further, all clouds below the level of complete attenuation are unreported. Because of the high forward-scattering nature of most cirrus, LITE penetrates all but the most optically-thick of these clouds. However, optically-thick stratus and clouds associated with deep convection have often been observed to attenuate the LITE signal completely.

Another phenomenon which leads to an underestimation of cloud base altitude is pulse stretching [*Winker and Poole*, 1995]. In-cloud multiple scattering of lidar photons results in temporal delay of the return signal; translating to a misranging of the cloud to distances farther away from the instrument. These stretched returns occur predominantly in

Table 1. Performance statistics computed for all LITE orbit cases. Parenthetical figures are allowances for ( ): ±1 bin in the horizontal and vertical, and [ ]: ±1 bin in the horizontal and ±2 bins in the vertical. See text for explanation of statistical fields.

Orbit	$\%_{MOD}$	$\%_{OBS}$	HR	TS	POD	FAR
079	0.224	0.264	0.858 (0.891) [0.923]	0.496 (0.660) [0.784]	0.549 (0.730) [0.875]	0.161 (0.127) [0.117]
083	0.302	0.314	0.880 (0.940) [0.946]	0.649 (0.854) [0.884]	0.690 (0.908) [0.948]	0.083 (0.065) [0.071]
085	0.233	0.287	0.794 (0.822) [0.836]	0.364 (0.558) [0.650]	0.425 (0.649) [0.760]	0.283 (0.201) [0.182]
115	0.274	0.278	0.854 (0.897) [0.912]	0.546 (0.713) [0.775]	0.612 (0.799) [0.876]	0.165 (0.130) [0.119]
116	0.296	0.358	0.851 (0.891) [0.923]	0.607 (0.753) [0.844]	0.643 (0.800) [0.902]	0.084 (0.072) [0.065]
123	0.423	0.371	0.838 (0.879) [0.903]	0.646 (0.779) [0.845]	0.726 (0.877) [0.958]	0.146 (0.125) [0.122]
124	0.376	0.315	0.867 (0.902) [0.921]	0.648 (0.785) [0.850]	0.726 (0.880) [0.960]	0.142 (0.120) [0.119]
128	0.114	0.222	0.877 (0.915) [0.935]	0.408 (0.624) [0.728]	0.418 (0.642) [0.755]	0.057 (0.044) [0.046]
129	0.191	0.191	0.888 (0.911) [0.925]	0.475 (0.642) [0.730]	0.562 (0.760) [0.866]	0.247 (0.194) [0.178]
131	0.258	0.269	0.873 (0.915) [0.940]	0.578 (0.765) [0.837]	0.635 (0.847) [0.952]	0.166 (0.112) [0.126]
134	0.314	0.286	0.846 (0.881) [0.893]	0.549 (0.707) [0.769]	0.627 (0.807) [0.884]	0.185 (0.149) [0.145]
145	0.216	0.274	0.864 (0.911) [0.928]	0.526 (0.729) [0.800]	0.569 (0.790) [0.869]	0.127 (0.095) [0.090]
148	0.224	0.188	0.887 (0.920) [0.944]	0.475 (0.680) [0.800]	0.547 (0.782) [0.929]	0.218 (0.161) [0.148]
149	0.369	0.241	0.862 (0.884) [0.907]	0.573 (0.701) [0.794]	0.663 (0.811) [0.927]	0.191 (0.163) [0.153]
150	0.392	0.325	0.840 (0.885) [0.899]	0.606 (0.759) [0.814]	0.682 (0.855) [0.925]	0.156 (0.129) [0.129]
TOT	0.289	0.284	0.859 (0.897) [0.916]	0.555 (0.721) [0.798]	0.621 (0.808) [0.900]	0.161 (0.129) [0.124]

water clouds while markedly less so in cirrus, owing again to differences in cloud optical properties [*Miller and Stephens,* 1998].

For these reasons, erroneous "false alarms" (due to pulse attenuation) and "misses" (pulse stretching) in our comparisons may occur in lower-level clouds and areas of deep convection. Although there presently exists no remedy to these problems other than to include them in a discussion of the intercomparison uncertainties, we demonstrate in this paper the utility of these data which nonetheless far exceed the capabilities of current satellite observing systems.

4. Work in Progress and Conclusion

This study comprises a subset of the research planned for the remote sensing validation of the ECMWF prognostic cloud scheme. The basic research goals are to determine i) the extent to which cloud information in operational models is adequate for prescribing cloud radiative feedback in the atmosphere, and ii) the likely impact of current remote sensing data on verifying and improving cloud analyses and cloud parameterization in models. Work in progress includes the use of satellite cloud property retrieval information to test the validity of model cloud bulk-microphysical properties. For interests of radiative transfer and cloud radiative feedbacks, both capacities (spatial and microphysical) must be satisfied. Identifying areas of model deficiency is of particular interest. Preliminary ensemble-orbit results, for example, indicate possible underestimation of the frequencey of high-altitude cirrus and overestimation of lower tropospheric cloud (subject to the caveats mentioned above). Processing of the remaining LITE orbits will build a more robust statistical database from which to better support or refute these inferred biases.

Demonstration of cloud prediction capabilities in GCMs opens the door to regarding reanalysis data as a heretofore overlooked source of valuable information to cloud feedback and cloud climatology studies. With the current level of model sophistication and validation data at our disposal, the time has come to address seriously this alluring possibility. Beyond assessing the skill of the current ECMWF prognostic cloud scheme, this study attempts to highlight the immediate windfall of a space-borne active-instrument observing system to the validation and further development of cloud prediction algorithms in GCMs.

Acknowledgments. The authors wish to thank Dave Winker and Mark Vaughan of NASA Langley Research Center for supplying the LITE data for this study. Funding for this research was provided by NASA Grant #NAG5-6637.

References

Cess, R. D., et al., Intercomparison and interpretation of climate feedback processes in 19 atmospheric general circulation models, *J. Geophys. Res., 95,* 16601-16615, 1990.

Jakob, C., The impact of the new cloud scheme on ECMWF's integrated forecasting system (IFS), *Proc. of ECMWF/GEWEX Workshop on Modelling, Validation and Assimilation of Clouds,* 277-294, 1994.

Klein, S. A., and C. Jakob, Validation and sensitivities of frontal clouds simulated by the ECMWF model, *Mon. Weather Rev.,* in press, 1998.

Lau, N. -C., and M. W. Crane, A satellite view of the synoptic-scale organization of cloud properties in midlatitude and tropical circulation systems, *Mon. Weather Rev.,* 1984-2006, 1995.

Mace, G. G., C. Jakob, and K. P. Moran, Validation of hydrometeor prediction from the ECMWF model during winter season 1997 using millimeter wave radar data. *Geophys. Res. Lett.,* in press, 1997.

McCormick, M. P., et al., Scientific investigations planned for the Lidar In-Space Technology Experiment (LITE), *Bull. Am. Meteorol. Soc., 74,* No. 2, 205-214, 1993.

Miller, S. D., and G. L. Stephens, Multiple scattering effects in the lidar pulse stretching problem, *J. Geophys. Res.,* in press, 1998.

Morcrette, J. -J., Evaluation of model-generated cloudiness: satellite-observed and model-generated diurnal variability of brightness temperature, *Mon. Weather Rev., 119,* 1205-1224, 1990.

Platt, C. M. R., and D. M. Winker, Multiple scattering effects in clouds observed from LITE, *Proc. SPIE, 2580,* 60-71, 1996.

Tiedke, M., Representation of clouds in large-scale models, *Mon. Weather Rev., 121,* 3040-3061, 1993.

Winker, D. M., and L. R. Poole, Monte-Carlo calculations of cloud returns for ground-based and space-based LIDARS, *Appl. Phys. B, 60,* 341-344, 1995.

Winker, D. M., and M. A. Vaughan, Vertical distribution of clouds over Hampton, Virginia observed by lidar under the ECLIPS and FIRE ETO programs, *Atmos. Res., 34,* 117-133, 1994.

Winker, D. M., R. H. Couch, and M. P. McCormick, An overview of LITE: NASA's Lidar In-space Technology Experiment, *Proc. IEEE, 84,* 164-180, 1996.

Wilks, D. S., *Statistical methods in the Atmospheric Sciences: An Introduction,* 427pp., Academic Press, San Diego, Calif., 1995.

A. C. M. Beljaars, European Centre for Medium-range Weather Forecasting, Shinfield Park, Reading, Berkshire RG2 9AX, England.

S. D. Miller and G. L. Stephens, Department of Atmospheric Science, Colorado State University, Ft. Collins, CO 80523.

(Received October 3, 1998; revised November 10, 1998; accepted December 10, 1998.)